Simulation of Food Solar Drying

Inês N. Ramos*, Teresa R.S. Brandão, Cristina L. M. Silva

CBQF- Centro de Biotecnologia e Química Fina, Escola Superior de Biotecnologia, Centro Regional do Porto da Universidade Católica Portuguesa
Rua Arquiteto Lobão Vital, Apartado 2511, 4202-401 Porto, Portugal

*Corresponding Author: iramos@porto.ucp.pt (Inês N. Ramos)

Abstract

This chapter discusses the simulation process of food solar drying, presenting the basic issues of mass and heat transfer under time-varying conditions. Food drying embraces several phenomena and scientists do not completely understand its underlying mechanisms. However, mathematical simulation and modelling provide comprehensions to improve the knowledge on the drying mechanisms, allow the prediction of the drying behaviour, as well as being essential tools in the design of solar drying equipment. The major difficulty in simulating food solar drying arises from variable meteorological conditions that change air temperature, moisture and velocity inside the solar equipment, during the drying process. Therefore, an integrated mass and heat transfer model under dynamic conditions is presented and appropriate assumptions are discussed. A meteorological model and desorption isotherms are taken into consideration as well. The integrated model includes food's shrinkage, changing boundary conditions and variable thermal properties and water diffusivity with time and space (non-isotropic characteristics).

Keywords:

Solar drying; Heat transfer; Mass transfer; Simulation; Modelling

1. Introduction

Exposing food products to the action of the sun is probably the oldest method of food preservation practiced by human civilisation. Removing water from the food product decreases microbial and enzymatic activities that originate quality decline and sometimes even product spoilage. Some early archaeological findings refer to far back as the Middle Bronze Age (21st to 17th centuries BCE) with dry and salted fish in ancient Egypt (Raban-Gerstel et al. 2008). With the Industrial Age, easier access to equipment and energy, new food drying technologies were developed, like spray drying, drum drying, fluidized bed drying, freeze-drying, etc. Presently, the demand for added-value dried products continues, but most of all environmental concerns in the society drive the development of eco-friendly and sustainable drying methods to produce minimal ecological and climate impact. Therefore, the improvement of solar drying techniques will play a role in a humanitarian and environmentally responsible society.

In solar drying, the temperature of the drying chamber is increased by using different methods to capture the solar energy (Fuller 1993). It is more hygienic than sun-drying (foods are exposed on the floor), since products are sheltered from rain, dust, insects and rodents. It also reduces drying time, preventing products spoilage by moulds due to the faster decrease of water activity. When compared to other drying techniques associated to sophisticated equipment, solar drying is relatively cheap, having smaller initial investment but requiring higher labour costs.

Considering the design of drying equipment, numerical simulation techniques are very useful, as they allow to minimize the investment of time, products and labour. Numerical simulation builds upon mathematical equations and appropriate boundary conditions, in order to generate a model which describes the drying process. Therefore, appropriate models are extremely important and their approach may be mechanistic or empirical. For an appropriate decision on the approach, a careful evaluation on benefits and drawbacks should be performed, also considering the main aim and availability of 'engineering parameters'. Empirical approaches are simpler and many times properly suitable for concrete purposes like the dryer' technical plan (Mulet 1994). On the other hand, mechanistic models are more complex and require more computational effort, but originate more accurate predictions. The borderline between mechanistic and empirical models is often not well defined, since mechanisms are themselves based on experimental observations (Mulet 1994). For an exhaustive and detailed review on thin-layer drying models of foods, please refer to Kucuk et al. (2014). Most solar drying process fall into the category of 'thin-layer drying', being this term used in opposition to deep-bed drying.

The fundamental drying mechanisms of foods are not easily perceived and not yet completely understood. Inside the product, various mechanisms of mass transfer were listed in a literature review on solids' drying (Waananen et al. 1993): liquid diffusion, vapour diffusion, surface diffusion, hydrodynamic or bulk flow and capillary flow. These mechanisms may occur simultaneously and modify their process percentage along drying.

A very useful tool in identifying drying mechanisms is the well-known 'characteristic drying curve', which is an experimental plot that depicts the drying rate as a function of water content. This plot allows distinguishing the different drying periods, being the most informative regarding the drying

process. The drying phases may be separated into constant-rate period and falling-rate period. Regarding food air-drying, the most common observation is a small constant-rate period and a longer falling-rate period (Mazza and Le Maguer 1980; Yusheng and Poulsen 1988; Mulet 1994; Madamba et al. 1996), until low values of equilibrium water content are reached. This observation may be attributed to the high density and low porosity of foods that originate slow drying and molecular diffusion of the water within the material is one of the main mechanisms (Mulet 1994). Therefore, many research works refer to Fick's second law to model the falling-rate period and Fickian models are the most widely applied in food drying.

The extra effort in simulating solar drying when compared to other drying processes is due to the great variability on meteorological conditions along the whole process, changing with the month of the year, hour of the day and weather conditions. This variability modifies air temperature, humidity and velocity inside the solar dryer, and typically produces a cyclic behaviour during the day. In a covered solar dryer, the incident radiation produces a greenhouse effect. It is the dryer' translucency that allows solar radiation to enter and be transmitted to the products inside, heating them. However, the heat emitted by the foods is not allowed to leave the dryer due to its extended wavelengths, increasing the dryer and food's temperature along the day.

An important aspect of foods' solar drying is shrinkage, although most of the mathematical models applied to solar drying until the eighties, ignored this important modification of product's characteristics (Ratti and Mujumdar 1997). Since then, methodologies have been upgraded in order to include shrinkage, meteorological aspects and time and space-varying mass and heat transfer properties. Some works have made significant contribution to one of these aspects, although not integrating all of them simultaneously (Youcef-Ali et al. 2001; Bennamoun and Belhamri 2006; Phoungchandang and Woods 2000).

The main objectives of this chapter are: i) to present the appropriate assumptions on heat and mass transfer mechanisms in a solar dryer, ii) to describe mass and heat equations for products inside a solar dryer and a meteorological model, iii) to review existing literature for moisture diffusivity equations of fruits, vegetables and cereals submitted to drying, iv) to incorporate in an integrated numerical model the previous equations plus product's shrinkage, variable mass diffusivity, variable thermal properties and boundary conditions, and v) to validate the integrated model with a case-study on grape drying in a mixed-mode solar dryer.

2. Modelling Assumptions

The modelling of solar drying processes must take into account both heat and mass transfer phenomena, simultaneously. The water transfer mechanism inside the solar dryer may be diffusional and convective, in the case of an existing fan. The heat transfer mechanism involves simultaneously convection, evaporation and radiation.

Some heat and mass transfer mechanisms may be considered negligible when compared to others, and therefore not accounted in the heat and mass balance equations. The criteria to make these assumptions are based on the analysis of the values of dimensionless numbers. For instance, to assess the relation between the resistance to heat transfer inside the product and at its surface, the Biot number (Bi) is used (Ramos et al. 2015) (Eq. 1). This dimensionless number expresses the

proportion between the resistance to heat conduction presented by the solid interior and the resistance to heat convection existing in the exterior fluid.

$$Bi = \frac{\bar{h}\, V/A_s}{Kp} \quad (1)$$

It is assumed that when the Bi number is less than 0.1, the effect of the internal impedance to heat transfer may be ignored, and consequently the material temperature is supposed to be isotropic in the entire food. An average product temperature is used in the models.

The same kind of logic may be applied to analyse the relation between internal and external resistance to mass transfer. The Biot number of mass transfer (Bi_m - Eq. 2) expresses the relation between internal resistance to diffusion and the external resistance to convection (Ramos et al. 2015).

$$Bi_m = \frac{h_D V/A_s}{D} \quad (2)$$

When the calculated value of the Bi_m is smaller than 0.1, the internal resistance to mass transfer can be ignored and the water content inside the product can be considered uniform. On the other hand, when Bi_m is higher than 10 the resistance to convection in the fluid is negligible, and therefore the air moisture around the food (inside the solar dryer) is supposed to be homogeneous. In this case, the average air moisture is used in the models. As referred before, in the mass transfer process inside the food product during the course of drying, diffusion is presumed to be the control mechanism.

3. Mass Transfer Model

In a situation where we have diffusion controlled drying, the Fick's second law may be applied. When dealing with spherical foods, the inner water content (X) at a given radial position (r) and time (t) can be calculated by equation 3 (Ramos et al. 2015).

$$\frac{\partial X_{r,t}}{\partial t} = \frac{1}{r^2}\frac{\partial}{\partial r}\left(D\, r^2 \frac{\partial X}{\partial r}\right) \quad (3)$$

For simplification purposes, water diffusivity may be considered independent of temperature (T) and water content. This is the most common approach in food drying modelling. Alternatively, for a more accurate numerical simulation, a water diffusivity equation may be integrated in the mass transfer models. A survey on existing literature for moisture diffusivity equations regarding fruits, vegetables and cereals submitted to drying processes is presented in Table 1, listing the drying method and food product used.

Table 1 Overview on models expressing water diffusivity dependence on temperature and water content, for fruits, vegetables and cereals.

Model	*Reference*	*Food / Drying method*
$D = a\,(-b + cX - d\,X^2)\exp(e\,T)$ (Eq.4)	(Jayas 1991)	wheat thin-layer

$D = \exp\left(a + \frac{b}{T} + c\,X\right)$	(Eq. 5)	(Mulet et al. 1989)	carrot convective
$D = a\ \exp\left(-\frac{b}{T}\right)\exp\left(-\frac{c}{X}\right)$	(Eq. 6)	(Maroulis et al. 1995)	potato convective
$D = a\exp\left[-\frac{b}{RgT}\left(\frac{c+\frac{1}{X}}{d+\frac{Ta-T}{X_0}}\right)\right]$	(Eq. 7)	(Kechaou and Maâlej 2000)	date convective
$D = \exp\left(a + b\,X + c\,X^2\right)$	(Eq. 8)	(Vázquez et al. 2000)	grape convective
$D = a\ \exp\left(-\frac{b}{RgT}\right)\exp\left(-cT - dX\right)$	(Eq. 9)	(Azzouz et al. 2002)	grape convective
$D = a + b\,X + c\,X^2 + d\,X^3$	(Eq. 10)	(Sharma and Prasad 2004)	garlic cloves micro-wave+convective
$D = D_0\ \exp\left[a\frac{X}{X_0} - b\left(\frac{X}{X_0}\right)^2 - c\left(\frac{1}{T} - \frac{1}{T_{av}}\right)\right]$	(Eq. 11)	(Ramos et al. 2010)	grapes convective

When solving Fick's second law, appropriate initial and boundary conditions must be selected. In a drying process, the boundary conditions are linked with the equilibrium water content – X_e. Water content at the product's surface is usually assumed in equilibrium with the air and is dependent on air humidity and temperature. When air conditions are time-varying, X_e is changing as well. Therefore, it is very important to determine X_e, which may be achieved using equations of moisture sorption isotherms, the curve representing the relationship between water activity and the water content of the product. These plots are very useful in dehydration processes, especially the desorption isotherm. There are numerous equations that mathematically represent these curves, being the most widely applied equations the following: Langmuir, Brunauer-Emmett-Teller (BET), modified Oswin, modified Halsey, modified Henderson, Chung-Pfost, Ferro-Fontan, Guggenheim–Anderson–deBoer (G.A.B.), Peleg, Timmermann-GAB, Viollaz-GAB and Lewicki (Basu et al. 2006). The G.A.B. model (Eq. 12) is the most popular since the eighties and it was more recently recommended based on statistical criteria, for fitting water sorption data in the extensive review of food isotherms by Basu et al. (2006).

$$\frac{Xe}{Xm} = \frac{C\,K\,a_w}{(1-K\,a_w)(1-K\,a_w + C\,K\,a_w)} \qquad (12)$$

4. Heat Transfer and Meteorological Model

The overall energy balance to a product exposed to solar drying, can be expressed in equation 13 (Phoungchandang and Woods 2000).

$$\frac{d(m\,Cp\,T)}{dt} = \alpha\,A_p I(t) - \bar{h}\,A_s(T - T_a) - \frac{d(\lambda\,m_w)}{dt} - A_s\,\varepsilon\,\sigma\,F(T^4 - T_a^4) \qquad (13)$$

This equation includes on its right member, four terms that correspond to the absorbed radiant energy and the heat lost by convection, evaporation and radiation, whose sum is equal to the energy added to the drying food (left member).

I(t) is the radiation flux density at a specific day time, and depends on meteorological conditions. The sampling time of radiation flux density should be as small as possible, or otherwise it may be reduced through suitable meteorological models. For instance, Charles-Edwards and Acock (1977) created a model that generates values of radiation flux density from global radiation values, considering the diurnal changes of radiation (Eq. 14). This equation is a complete sine wave and the original purpose of its authors was to mathematically define diurnal variation in photosynthetically active radiation.

$$I(t_d) = \begin{cases} \dfrac{J_N}{g_N}\left\{1+\cos\left[\dfrac{2\pi}{g_N}\left(t_d-0.5\right)\right]\right\} & ; \quad 0.5-\dfrac{1}{2}g_N \le t_d \le 0.5+\dfrac{1}{2}g_N \\ 0 & ; \quad \text{otherwise} \end{cases} \tag{14}$$

J_N represents the global radiation corresponding to day N, g_N the daylength, varying between zero and one and t_d represents the time normalization of one day period, *i.e.*, $t_d = \dfrac{t(h)}{24} \quad (0 < t_d < 1)$. Midnight corresponds to t_d =0.

In order to calculate the daylength (g_N – Eq. 15) it is necessary to determine two other meteorological parameters; the solar declination (δ - Eq. 16) and the year angle (y – Eq. 17).

$$g_N = \frac{2\arccos\left(-\tan\phi\tan\delta\right)}{2\pi} \tag{15}$$

$$\delta = 0.38092 - 0.76996\cos(y) + 23.26500\sin(y) + 0.36958\cos(2y) + 0.10868\sin(2y) + 0.01834\cos(3y) - \\ - 0.16650\sin(3y) - 0.00392\cos(4y) + 0.00072\sin(4y) - 0.00051\cos(5y) + 0.00250\sin(5y) + 0.00442\cos(6y) \tag{16}$$

$$y = \left(\frac{N-21}{365}\right)2\pi \tag{17}$$

In equation 17, N symbolises the climatological day number (the first day of May corresponds to N=1) and ϕ is the latitude of the location of the solar dryer.

5. Integrated Numerical Methodology

Most partial differential equations do not have an analytical solution and therefore discretization methods are needed (sometimes using a numerical grid), aiming at its transformation into a system of algebraic equations. Using a computer program, these equations are solved and originate values on time and space dimensions. Numerical techniques in solar drying developed from simpler and faster approaches such as finite-differences, finite-elements, finite-volumes, to more complex and time-

consuming methodologies such as computational fluid dynamics (CFD) softwares, artificial neural network, fuzzy modelling, etc.

The methodology presented below applies to drying of spherical products in a mixed mode or hybrid cabinet dryer. The forward explicit finite differences method was chosen to numerically solve Fick's second law applied to a spherical material (Eq. 3) and the energy balance equation (Eq. 13). If time and space derivatives of both equations are discretised, equations 18 and 20 are respectively obtained.

$$X_i^{t+1} = X_i^t\left(1 - 2\frac{\Delta t\, D_i^t}{\Delta r^2}\right) + X_{i+1}^t\left(\frac{\Delta t\, D_i^t}{\Delta r^2} + \frac{\Delta t\, F_i^t}{2\Delta r}\right) + X_{i-1}^t\left(\frac{\Delta t\, D_i^t}{\Delta r^2} - \frac{\Delta t\, F_i^t}{2\Delta r}\right) \quad (18)$$

being $$F_i^t = \frac{1}{r_i^2}\frac{D_{i+1}^t\, r_{i+1}^2 - D_{i-1}^t\, r_{i-1}^2}{2\Delta r} \quad (19)$$

$$T_{t+1} = T_t + \left[\alpha\, A_p(X_t)\, I(t) - \bar{h} A_s(X_t)(T_t - Ta) - \frac{\lambda\,(X_t - X_{t+1})\, m_0}{\Delta t\ (1+X_0)} - A_s(X_t)\,\varepsilon\,\sigma\, F(T_t^4 - Ta^4)\right]\frac{(1+X_0)\ \Delta t}{Cp\, m_0\,(1+X_t)} \quad (20)$$

The space domain has to be divided into a given number of nodal points. F in equations 13 and 20 is a geometry factor and is usually considered equivalent to 1, when dealing with small bodies inside large areas (Ramos et al. 2015).

The following initial and boundary conditions were applied: i) uniformity (isotropicity) of the water content in the whole product for the initial drying time, ii) "water content at the surface of the product always in equilibrium with the surrounding air" (Ramos et al. 2010) and is stable over time, and iii) a symmetric condition for the water content at the food's centre, indicating there is no water flow in this point.

i) $t = 0$, $0 \le r \le R$ $\quad X = X_0$

ii) $t \ge 0$, $r = R(t)$ $\quad X_R = Xe(t)$

iii) $t \ge 0$, $r = 0$ $\quad \frac{\partial X}{\partial t} = 0$

This was a moving boundaries process, with changes in external dimensions of the product (R) due to shrinkage along drying, and modifications in the values of equilibrium moisture content (Xe), for being subjected to changing air conditions (Ramos et al. 2010).

The flowchart presented in Figure 1 is a proposed integrated methodology for the numerical simulation of solar drying curves of food (Ramos et al 2015). This methodology takes shrinkage of the product into account, including modifications on its surficial area and projected area.

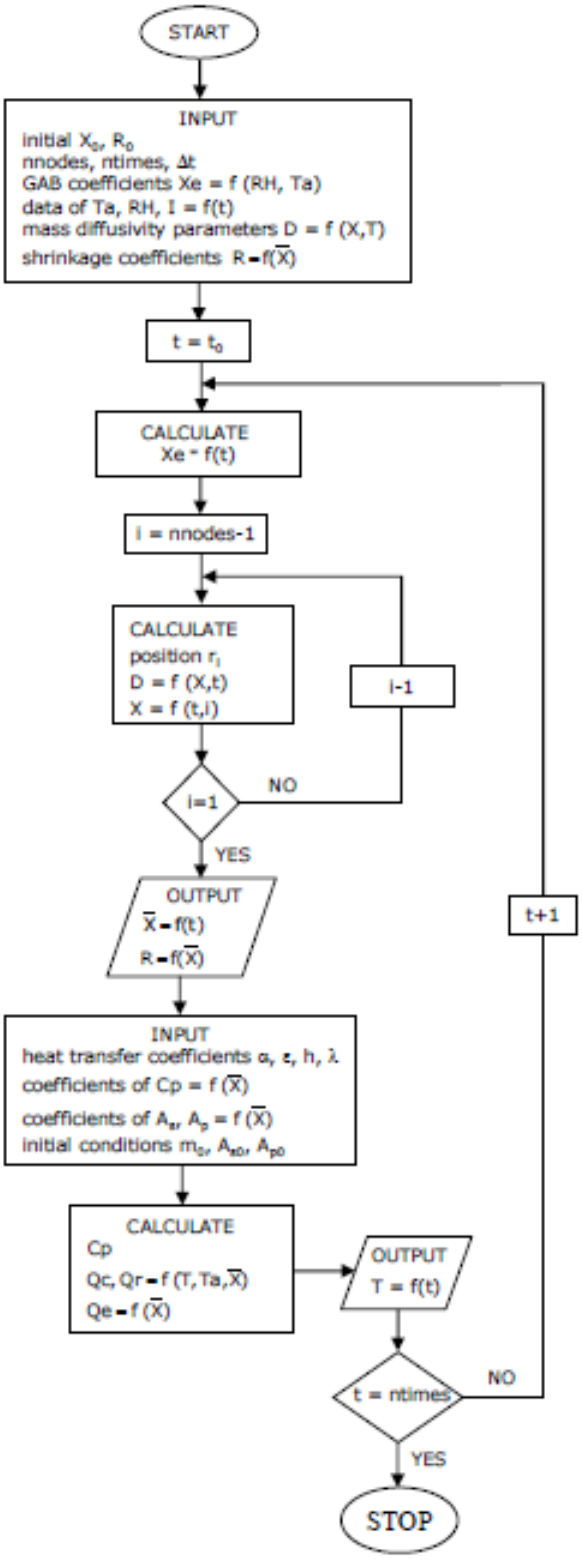

Figure 1. Flowchart of the integrated simulation.

It also considers some anisotropic characteristics of the food; modifications in effective moisture diffusivity with water content and temperature, and changes in thermal properties of grapes.

The first input data on the flowchart are initial X_0 and R_0 values of the food, shrinkage coefficients regarding the radius, the equilibrium coefficients for the GAB model, water diffusivity coefficients (D_0,

a, b, c), number of nodes, number of time steps and time interval (later presented in Table 2). Air conditions (temperature and relative humidity) and radiation flux density, are introduced in the flowchart as well. The next command is an external loop executed for every drying time step. The first calculation is the equilibrium water content and then an internal loop to determine the position of the nodes in the product and the corresponding particular water content at every node, with changing water diffusivity. The next step is the output of the average water content determined by integration with the trapezoidal rule, and the corresponding new food radius at each drying time. The last input is the heat transfer coefficients, shrinkage parameters of A_s and A_p and their initial values and initial total mass. And finally, the convective heat loss (Qc), the evaporative heat loss (Qe), the radiation heat loss (Qr) and the specific heat are calculated. The last output is the determined food temperature.

6. Case Study

This case study was conducted in a field solar drier located in the northern region of Portugal (Mirandela), using grapes as raw material. Solar dryers may be classified into direct, indirect, mixed mode or hybrid, according to Fuller (1993). This dryer classifies as a mixed mode or hybrid cabinet dryer, and includes “a collector for pre-heating the air, a drying chamber and a solar chimney” (Ramos et al. 2015). Two exhaust air fans are included on the back wall and it has a continuous 30 cm opening for air admission. The dryer collector faces south, as is usual in the North hemisphere, in order to take full advantage of solar radiation and makes an angle of 38°, being identical to the local latitude (ϕ) of 41.28 °N.

Red seedless grapes from the cultivar *Monukka* were used. Whole grape clusters were reduced to smaller portions and blanched in hot water for around 15 seconds. Around 5 kg of blanched grapes were placed in each wood tray of the solar dryer, totalizing an initial load of approximately 250 kg. Samples were collected from different locations on the dryer and drying was performed until reaching a constant weight.

Air temperature and relative humidity inside the dryer were recorded every 15 minutes. As expected, the air temperature increased from dawn until sunset, in the range 12–42^{o}C, and relative humidity in the range 8–86%. Air velocity was determined in the initial and final rows of the solar dryer twice a day, and values varied between 9 and 34 cm s^{-1}. Meteorological data from the region (daily values of global radiation, J_N) were collected from the Portuguese meteorological institute. They were later transformed to hourly data of radiation flux density $I(t_D)$ for each drying day, using the Charles-Edwards and Acock model (Eq. 14) and included as input data in the integrated numerical simulation. These data (Figure 2) present a daily variation with a sinusoidal pattern, which corresponds to day rise of air temperature and night decline and respective opposite, decline and rise of air relative humidity.

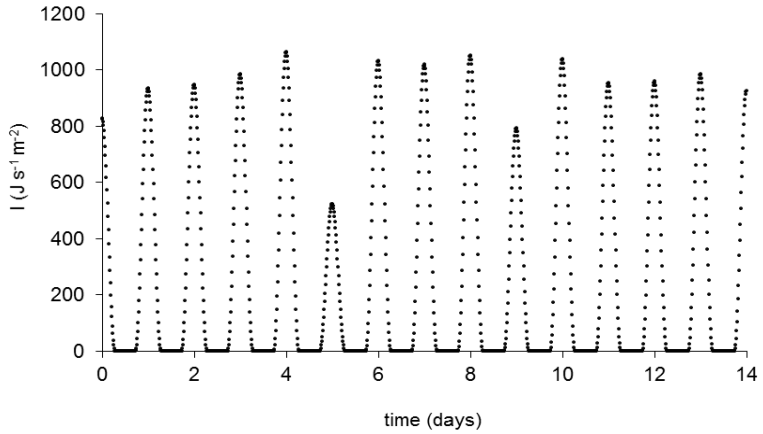

Figure 2. Radiation flux density calculated with Charles-Edwards and Acock equations.

The integrated simulation methodology allowed the estimation of drying curves. A typical example is presented in Figure 3, as well as a set of experimental data acquired in the mixed-mode solar dryer.

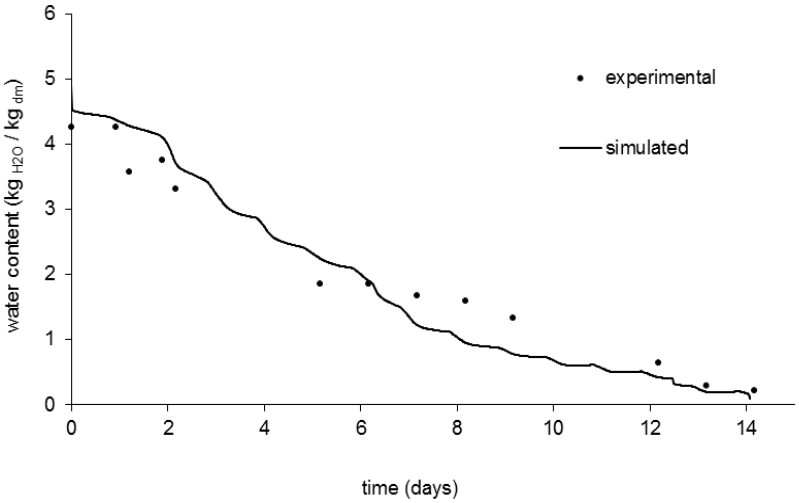

Figure 3. Simulated drying curve (continuous line) and experimental data from the mixed-mode solar dryer (●).

Good estimations of the experimental curves were attained, considering the small number of experimental data and the high variability on their values. Steps are observed in the simulation values, which are linked to the sinusoidal cyclic pattern of day and night meteorological conditions.

Table 2 presents coefficients and equations used in the numerical simulation: water diffusivity of grapes and heat transfer parameters, shrinkage equations and equilibrium GAB coefficients. A previous study on grape convective drying at pilot scale (Ramos et al. 2010) provided the estimations range for the input of the parameters of the diffusivity model (D_0, a, b, c). The best adjust to experimental data corresponded to deviations of input values from original estimated values of 70, 4, 8 and 65%, respectively for D_0, a, b, and c parameters. These values fall within acceptable confidence intervals of the estimates.

Table 2 Coefficients and equations used in the simulation

Mass diffusivity parameters (Ramos et al. 2010) (Eq. 11)
$D_0 = 5 \times 10^{-12}$ m^2 s^{-1}
a = 15
b = 25
c = 2200 K
T_{av} = 303.15 K
Heat transfer parameters
$\bar{h}$ = 1.263 W m^{-2}°C
λ= 2419 kJ kg^{-1}
ε = 0.73
α = 0.823
$Cp = 1.3767 - 3.181 \times 10^{-3} T + 2.9293$ W (J kg^{-1} K^{-1})
$Kp = -0.022 + 1.924 \times 10^{-3} T + 0.587$ W (J kg^{-1} K^{-1})
Shrinkage equations (Ramos et al. 2010)
$R = R_0 \left(0.3654 \ \frac{\bar{X}}{X_0} + 0.6288 \right)$
$A_p = A_{p0} \left(0.6314 \ \frac{\bar{X}}{X_0} + 0.3521 \right)$
$A_s = A_{s0} \left(0.5627 \ \frac{\bar{X}}{X_0} + 0.4054 \right)$
$R_0 = 0.75 \pm 0.07$ cm
A_{p0} = 1.01 m^2
A_{s0} = 2.16 m^2
GAB coefficients for Muscatel raisins (Vázquez et al. 1999)
$C = C_0 \exp\left(\frac{H_1 - H_m}{Rg\ T} \right)$ $\qquad$ $K = K_0 \exp\left(\frac{H_1 - H_q}{Rg\ T} \right)$
Xm=0.119
C_0 =0.107
$(H_1-H_m)/Rg$ = 561.66
K_o = 0.911
$(H_1-H_q)/Rg$ = 9.07

7. Conclusions and Recommendations

Mathematical simulation and modelling are crucial to predict the drying behaviour, to design the solar drying equipment, and are valuable tools to improve the knowledge on the fundamental mechanisms of drying. Numerical simulation also allows to calculate drying times and subsequently optimising drying loads and planning the production of dried foods.

The simulation methodology presented in this chapter considers a dynamic process, integrating heat and mass transfer, food's shrinkage during drying, changing thermal properties and water diffusivity along drying and within the product, variable boundary conditions and sorption isotherms. This methodology may be coupled with the heat transfer model of the whole solar dryer, obtaining a complete simulation that originates directly from meteorological data. It may be applied to simulate solar drying of other innumerable foods, besides grapes, assuming the availability of their specific characteristics.

Furthermore, the integrated model can also be enlarged to a three-dimensional model, taking into account irregular shape (like wrinkles) and anisotropic shrinkage, having all space variables varying with time. The simulation can be carried out with other diffusivity and thermal properties equations that consider water content and temperature effects.

Integrative dynamic simulations that take simultaneously into account anisotropic transient characteristics and different mass and heat transfer mechanisms, should lead the way to progress on describing the drying process. The last years' improvement of knowledge on other drying scales like microscopic, should permit taking the path into more precise and accurate simulations.

Acknowledgements

Inês N. Ramos and Teresa R. S. Brandão gratefully acknowledge Fundação para a Ciência e a Tecnologia (FCT) and European Social Fund (ESF) the financial support through the Post-Doctoral grants SFRH/BPD/75430/2010 and SFRH/BPD/101179/2014, respectively. This work was also supported by National Funds from FCT through project UID/Multi/50016/2013.

Nomenclature

a, b, c, d, emodel parameters

a_w water activity

A_p projected area of the product (m^2)

A_s surface area of the product (m^2)

Bi Biot number

Bi_m Biot number for mass transfer

C Guggenheim constant

C_0, K_0 pre-exponential factors of C and K of equation 13 and table 2

Cp specific heat of the product (J kg^{-1} K^{-1})

D moisture diffusivity (m^2 s^{-1})

D_0 pre-exponential parameter of moisture diffusivity (m^2 s^{-1})

F geometry factor

g_N daylength

$\bar{h}$ average convective heat transfer coefficient (J s^{-1} m^{-2} K^{-1})

h_D convective mass transfer coefficient (m s^{-1})

H_1, H_m, H_q parameters of C and K of equation 13 and table 2

i node

I radiation flux density (J s^{-1} m^{-2})

J_N global radiation in the N^{th} day (J m^{-2})

K factor that corrects properties of the multilayer molecules with respect to the bulk liquid

Kp thermal conductivity of the product (W m^{-1} $°C^{-1}$)

m total mass of the product (kg)

m_w mass of evaporated water (kg)

N climatological day number

Qc convective heat loss (J s^{-1})

Qe evaporative heat loss (J s^{-1})

Qr radiation heat loss (J s^{-1})

r radial position

R average equivalent radius (m)

Rg universal gas constant (8.314 J mol^{-1} K^{-1})

t time (s or min)

t_d fractional part of a day time

T product temperature (K)

T_a air temperature (K)

V volume (m^3)

$\bar{X}$ average water content on dry basis (kg_{water} $kg_{dry\ matter}^{-1}$)

X water content on dry basis (kg_{water} $kg_{dry\ matter}^{-1}$)

Xe equilibrium water content on dry basis (kg_{water} $kg_{dry\ matter}^{-1}$)

Xm monolayer water content (kg_{water} $kg_{dry\ matter}^{-1}$)

y	year angle

Greek symbols

α	absorptivity of solar radiation
δ	solar declination
Δt	time interval (s)
Δr	space interval (m)
ε	emissivity
λ	latent heat of vaporization (J kg^{-1})
ϕ	latitude (°)
σ	Stefan-Boltzmann constant (5.6704×10^{-8} W m^{-2} K^{-4})

Subscripts

0	initial value
av	average value
r	at radius r
t	at time t

References

Azzouz S, Guizani A, Jomaa W, Belghith A (2002) Moisture diffusivity and drying kinetic equation of convective drying of grapes. J Food Eng 55: 323-330

Basu S, Shivhare US, Mujumdar AS (2006) Models for sorption isotherms for foods: a review. Dry Technol 24: 917-930

Bennamoun L, Belhamri A (2006) Numerical simulation of drying under variable external conditions: Application to solar drying of seedless grapes. J Food Eng 76(2):179-187

Charles-Edwards DA, Acock B. (1977) Growth response of a chrysanthemum crop to the environment. II a mathematical analysis relating photosynthesis and growth. Ann. Bot. 41-49.

Fuller RJ (1993) Solar drying of horticultural produce: Present practice and future prospects. Postharvest News Inform 4(5): 131N-136N

Kechaou N, Maâlej M (2000) A simplified model for determination of moisture diffusivity of date from experimental drying curves. Drying Tech 18(4,5): 1109-1125

Kucuk H, Midilli A, Kilic A, Dincer I (2014) A Review on Thin-Layer Drying-Curve Equations, Dry Technol 32(7): 757-773

Madamba PS, Driscoll RH, Buckle KA (1996) The thin layer drying characteristics of garlic slices. J Food Eng 29: 75-97

Maroulis ZB, Kiranoudis CT, Marinos-Kouris D (1995) Heat and mass transfer modeling in air drying of foods. J Food Eng 26: 113-130

Mazza G, Le Maguer M (1980) Dehydration of onion: some theoretical and practical considerations. J Food Technol 15: 181-194

Mulet A, Berna A, Rosselló C (1989) Drying of carrots. I. Drying models. Dry Technol 7(3): 537-557

Mulet A (1994) Drying modelling and water diffusivity in carrots and potatoes. J Food Eng 22: 329-348

Jayas DS, Cenkowski S, Pabis S, Muir WE (1991) Review of thin-layer drying and wetting equations. Dry Technol 9(3): 551-588

Phoungchandang S, Woods JL (2000) Solar drying of bananas: mathematical model, laboratory simulation, and field data compared. J Food Sci 65(6): 990-996

Raban-Gerstel N, Zohar I, Bar-Oz G, Sharon I, Gilboa A (2008) Early Iron Age Dor (Israel): A Faunal Perspective. B Am Sch Oriental Re 349: 25-59

Ramos IN, Miranda JMR, Brandão TRS, Silva CLM (2010) Estimation of water diffusivity parameters on grape dynamic drying. J Food Eng 97(4): 519-525

Ramos IN, Brandão TRS, Silva CLM (2015) Simulation of solar drying of grapes using an integrated heat and mass transfer model. Renew Energ 81: 896-902

Ratti C, Mujumdar AS (1997) Solar drying of foods: modeling and numerical simulation. Sol Energy 60(3,4): 151-157

Sharma GP, Prasad S (2004) Effective moisture diffusivity of garlic cloves undergoing micro-wave-convective drying. J Food Eng 65(4): 609-617

Vázquez G, Chenlo F, Moreira R, Carballo L (1999) Desorption isotherms of muscatel and aledo grapes, and the influence of pretreatments on muscatel isotherms. J Food Eng 39(4): 409-414

Vázquez G, Chenlo F, Moreira R, Costoyas A (2000) Effects of various treatments on the drying kinetics of Muscatel grapes. Dry Technol 18(9): 2131-2144

Waananen KM, Litchfield JB, Okos MR (1993) Classification of drying models for porous solids. Dry Technol 11(1): 1-40

Youcef-Ali S, Messaoudi H, Desmons JY, Abene A, Le Ray M (2001) Determination of the average coefficient of internal moisture transfer during the drying of a thin bed of potato slices. J Food Eng 48(2): 95-1

Yusheng Z, Poulsen KP (1988) Diffusion in potato drying. J Food Eng 7: 249-262